Available online at www.sciencedirect.com

ScienceDirect

IFAC Papers Online CONFERENCE PAPER ARCHIVE

IFAC PapersOnLine 56-2 (2023) 3170–3177

Towards Real-Time Combustion Phase Estimation for linear RCCI Model-Predictive Control Design

Amin Modabberian * **Xiaoguo Storm** ** **Aneesh Vasudev** ** **Kai Zenger** *
Jari Hyvönen *** **Maciej Mikulski** **

* *Aalto University, School of Electrical Engineering, Department of Electrical Engineering and Automation, Maarintie 8, 02150, Espoo, Finland (e-mail: firstname.lastname@aalto.fi)*
** *University of Vaasa, School of Technology and Innovations, Energy Technology, Yliopistonranta 10, 65200 Vaasa, Finland (e-mail: firstname.lastname@uwasa.fi)*
*** *Engine Research and Technology Development at Wärtsila Marine Solutions, Vaasa, Finland (e-mail: firstname.lastname@wartsila.com)*

Abstract: Reactivity controlled compression ignition (RCCI) technology has gained in popularity due to its ability to achieve low level NO_x and soot emissions with relatively high brake thermal efficiency. However, control of RCCI combustion is a complex task. Nonetheless, this challenge can be overcome with model-based control design (MBCD). In this work, a linear physics-based time-varying RCCI combustion model was developed and improved with an addition of a start-of-combustion (SOC) model. The model we developed, which is capable of real-time simulations, can predict the combustion phasing, heat-release, and cylinder pressure of an RCCI marine engine. The model showcases the trend-wise, high accuracy estimation of cumulative heat-release and cylinder pressure. Additionally, it is able to predict combustion phasing parameters with an error of less than 1% for control design.

Keywords: start of combustion, auto-ignition, real-time modelling, control-oriented model, RCCI, MPC

1. INTRODUCTION

There has been a growing interest in the utilization of dual-fuel reactivity controlled compression ignition (RCCI) technology for the next generation of combustion engines (Mikulski et al., 2019) in the marine and off-road sectors. The appeal is driven by ultra low levels of soot and NO_x ($<$ 0.01 and 0.5g/kWh, respectively [Benajes et al., 2015]), reported thermal efficiency in excess of 55% (Splitter et al., 2011), a direct 25% reduction in CO_2 footprint with biofuels (Arnberger et al., 2018), and retrofitability. While the aforementioned are proven benefits (Reitz and Duraisamy, 2015), certain issues remain regarding the practical adoption of this technology. In terms of controller development, the challenges include:

i. the lack of a direct ignition trigger, due to inherent chemical kinetics of limited heat-release, thereby making the process highly sensitive to conditions at the inlet valve closing (IVC)

ii. constraints to the operating envelope caused by excessive cylinder pressures (P_{max}), the pressure rise rates (PRR_{max}), engine out emissions (particularly unburned hydrocarbons [UHC] [De Ojeda et al., 2012])

iii. combustion stability issues and difficult transients

iv. challenging calibration stemming from the large number of control parameters, including the fuel blend ratio (BR), injecting timing, excess air coefficient (λ), and valve timings

Thus, the requirements of a robust controller that can scale with hardware and operational constraints and systematically handle a multiple-input and multiple-output (MIMO) cross-coupled system, call for model predictive control (MPC) methodology.

Thus far, MPC applied to RCCI has focused on combustion phasing and load control within prescribed combustion boundaries. Implementations of embedded real-time control-oriented models (COM) include linearized white-box quasi-empirical phenomenological models (Raut et al., 2018) and, fast black-box data-driven to grey-box models (Irdmousa et al., 2021, 2019; Basina et al., 2020). Linearized white-box approaches are computationally heavy, with limited applicable range and fidelity, while data-driven approaches require a large amount of data and suffer from concept transfer (Albin Rajasingham, 2021). In addition, these approaches are unable to provide high frequency in-cycle combustion details. Thus, the ultimate goal of our current research is to develop a real-time COM (RTM) for RCCI-MPC that provides detailed combustion insights and is computationally fast, robust, and predictive over a broad operating range. The current paper contributes to this goal by providing the first demonstration a linear physics-based time-varying state-space RTM (Storm, 2023) improved with the inclusion of a start-of-combustion (SOC) model. Ultimately, the combined model meets the aforementioned requirements with its rich output and fast computation, demonstrates high reliability and fidelity in boundary condition prediction, and, further, systematically improves autonomy.

⋆ This research is part of the Clean Propulsion Technologies -project (CPT) funded by Business Finland. The experimental data was provided by Wärtsilä Oyj Abp

10.1016/j.ifacol.2023.10.1452

2. METHODOLOGY

Development of the COM is based on a higher-order, experimentally validated, physics-based model called the University of Vaasa Advanced Thermo-kinetic Multizone Model (UVATZ), developed by Vasudev et al. (2022a). The novel cycle-based real time model (RTM) is a physics-based time-varying linear state-space model, potentially suitable for MPC implementation. The model is used as a predictive model for MPC to control blend ratio of fuels and the total fuel energy. The original RTM is equipped with a cumulative heat-release (CHR) curve shifting function using a tunable parameter. In this work, this shifting function is replaced by a physics-based SOC model, which considerably improves RTM autonomy and reliability. Both the SOC model and the coupled SOC and RTM are calibrated and validated thoroughly against the UVATZ model, as shown in Fig. 1. The details of the RTM and SOC models are presented in sections 2.1 and 2.2, respectively. The framework of this work is outlined in Fig. 1.

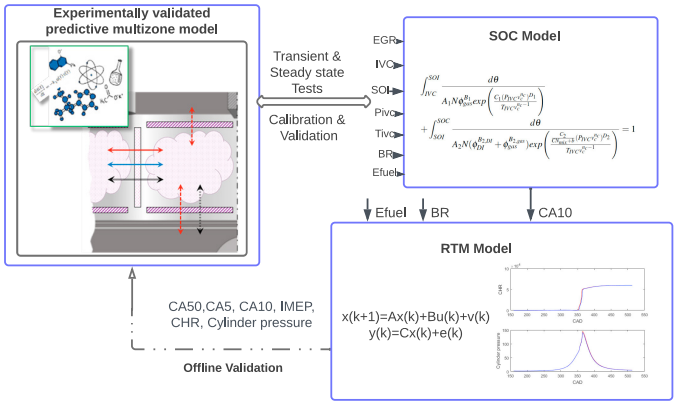

Fig. 1. Work outline and process

2.1 RTM

The RTM follows the general framework proposed by Turesson (2018) for partially premixed combustion (PPC) control. In its original context, the methodology was experimentally proven to be able to replicate crank angle resolved pressure and heat-release with real-time simulation capability and high accuracy. BR and total fuel energy (E_{fuel}), which were obtained from a previously conducted sensitivity study and literature review (Raut et al., 2018; Irdmousa et al., 2021) are used as control variables. The cycle-by-cycle RTM extends the method from Turesson (2018) to the RCCI concept with the assumption that small control input changes result in small CHR variation. The next cycle's CHR and cylinder pressure (P) are the sum of the previous cycle's CHR plus the induced changes from the E_{fuel} and BR with respect to $\frac{dCHR}{dE_{fuel}} = \frac{CHR}{E_{fuel}}$ and $\frac{dCHR}{dBR} = \frac{CHR}{BR}$. The details of the RTM linearization methodology are illustrated in an ongoing paper (Storm, 2023).

$$CHR(k+1) = CHR(k) + \frac{dCHR}{dE_{fuel}}\Delta E_{fuel}(k) + a_1\frac{dCHR}{dBR}\Delta BR(k) \quad (1)$$

$$P(k+1) = P(k) + \frac{dP}{dE_{fuel}}\Delta E_{fuel}(k) + a_2\frac{dP}{dBR}\Delta BR(k) \quad (2)$$

$$BR = \frac{m_{NG}LHV_{NG}}{m_{NG}LHV_{NG} + m_{LFO}LHV_{LFO}} \quad (3)$$

With E_{fuel} and BR increasing, the next cycle's CHR magnitude will increase accordingly, as shown in Fig. 2.

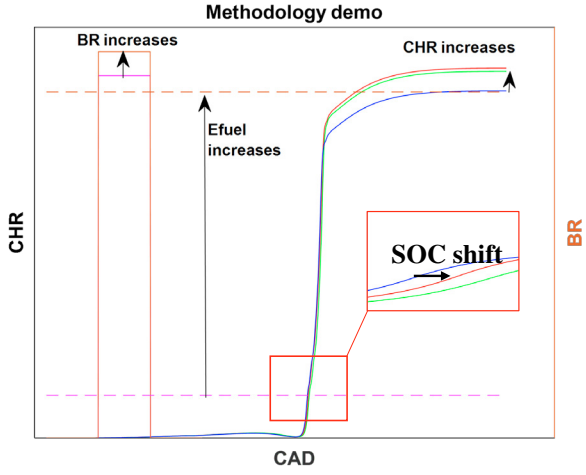

Fig. 2. RTM methodology demo. CHR is proportional to the changes of BR and E_{fuel}. Increasing the SOC shifts the CHR trace to the right, and decreasing the SOC shifts the trace to the left.

The calculated CHR curve is further shifted along the crank angle axis, as highlighted in the zoomed-in window from Fig. 2, according to predefined tuning parameters. These are defined in table 1.

Table 1. Used parameter constants

ΔE_{fuel}	ΔBR	BR(k+1)	ΔSOC	ΔSOC shifting
0	+1	$\leq BR_{change}$	R	A
+1	0	–	L	A
+1	+1	$\leq BR_{high}$	R	1
+1	+1	$\geq BR_{high}$	L	1

R: CHR shifts to the right, *L*: CHR shifts to the left, A: shifting CAD

Here BR_{change} and BR_{high} are general parameters that indicate the combustion behavior changing point. In this work, they are defined as an IMEP-axis 1-D table from 1 to 20 bar. The linear interpolation limit for BR_{high} is from 0.8 to 0.98 and for BR_{change} from 0.55 to 0.91. A is defined as a 1-D tuning table based on BR from 0.73 to 0.93 with shifting interpolated from 0.2 to 3.8 CAD. The coefficients a_1 and a_2 are tuning parameters, which will be defined in details in Storm (2023).

2.2 SOC model

Auto-ignition has been a constituted a particular area of interest among research communities, and several methods have been developed throughout the years, ranging white-box to gray-box modeling. For example, Kakoee et al. (2020) utilized a modified knock integral method and Wiebe functions to estimate SOC, CA50 and IMEP on a heavy-duty engine. Mishra and Subbarao (2021) developed a hybrid control model to estimate SOC, CA50, and P_{max} utilizing a modified knock integral model, an extended Wiebe function and artificial neural networks. In addition, Sadabadi et al. (2016) developed a full dynamic RCCI model for control application. The model estimates combustion parameters utilizing the Livengood-Wu integral, the

Wiebe function, and a spontaneous ignition front-speed-based burn-duration model. Moreover, Kondipati et al. (2017) further developed the same model towards steady-state and transient cases and used a PI-controller to control the injection timing and blend ratio of the fuels to reach the desired combustion phasing level. Raut et al. (2018), in turn, further extended the previous approach of Kondipati et al. (2017) to control the same parameters with a linear quadratic integral (LQI) controller and MPC.

The current work uses a modified knock-integral model (MKIM) (Sadabadi, 2015) to predict the start of combustion. The model is an auto-ignition model developed for RCCI process and based on the works of Livengood and Wu (1955) and Shahbakhti (2009). Livengood and Wu (1955) developed the knock-integral model (KIM) to predict auto-ignition in SI-engines. Shahbakhti (2009) further extended the same model towards HCCI combustion concept.

The SOC of RCCI is dependent on the conditions at IVC, injection timing, the equivalence ratio, the blend ratio of the fuels, and exhaust gas recirculation (EGR) (Sadabadi, 2015). The MKIM is presented in (4)

$$\int_{IVC}^{SOI} \frac{d\theta}{A_1 N \phi_{LRF}^{B_1} exp\left(\frac{C_1 (P_{IVC} v_c^{n_c})^{D_1}}{T_{IVC} v_c^{n_c-1}}\right)} + \int_{SOI}^{SOC} \frac{d\theta}{A_2 N (\phi_{HRF}^{B_{2,HRF}} + \phi_{LRF}^{B_{2,LRF}}) exp\left(\frac{\frac{C_2}{CN_{mix}+b} (P_{IVC} v_c^{n_c})^{D_2}}{T_{IVC} v_c^{n_c-1}}\right)} = 1 \tag{4}$$

In Equation (4), A_1, B_1, C_1, D_1, A_2, $B_{2,LRF}$, $B_{2,HRF}$, C_2, b and D_2 are tuning coefficients, such that the condition of the equation holds. Moreover, N is the engine speed, ϕ is the equivalence ratio of high and low reactivity fuel (HRF, LRF), P_{IVC} and T_{IVC} are pressure and temperature at IVC, n_c is the polytropic compression coefficient, CN_{mix} describes the reactivity of the fuel blend and v_c is the ratio of volume at IVC to the volume at any crank angle. CN_{mix} and v_c are defined in (5) and (6) respectively

$$CN_{mix} = \frac{FAR_{st,HRF}\phi_{HRF}CN_{HRF} + FAR_{st,LRF}\phi_{LRF}CN_{LRF}}{FAR_{st,HRF}\phi_{HRF} + FAR_{st,LRF}\phi_{LRF}} \tag{5}$$

$$v_c = \frac{V(\theta_{IVC})}{V(\theta)} \tag{6}$$

In Equation (5), FAR_{st} is the fuel-to-air ratio, ϕ is the equivalence ratio and CN is the cetane number of the fuels, respectively.

The integral from IVC to start of injection (SOI) deals with the compression of LRF, while the integral from SOI to SOC deals with compression of the mixture of LRF and HRF. More details about the model can be found in Sadabadi (2015).

2.3 RTM embedded with the SOC model

The main contribution of this work is to improve the RTM shifting function such that manual tuning and shifting are replaced by an automated and systematic process. Shifting is estimated by the MKIM described in section 2.2, which estimates the SOC of the next cycle. Here, CA10 is used as reference for SOC because the kinetic nature of the combustion and CA05 contain a large degree of uncertainty. The SOC of current cycle, $SOC(k+1)$, is compared to the SOC of the previous cycle, $SOC(k)$, and the shifting of CHR is performed according to the difference of the SOC values between the cycles as described in (7):

$$N = \frac{SOC(k+1) - SOC(k)}{Resolution} \tag{7}$$

The calculated N provides both the shifting number and the direction. For instance, when N is smaller than zero, it indicates an earlier SOC. Thus, it is shifted left. Similarly an N greater than zero indicates a right shift, while an N equal to zero means no shift. In this way, the system will automatically shift in the correct direction. Thus, the combined RTM and SOC model can provide a systematic means of CA10 and CA50 estimation. Cylinder pressure and the IMEP are not directly related. Therefore, analysis is focused on CA10 and CA50 in this paper.

2.4 Source of reference data

The data required for calibration and validation is obtained from the UVATZ model introduced at the beginning of section 2. UVATZ captures the effects of fuel injection and mixing, in-cylinder heat and mass flows, and wall heat loss on the ensuing heat-release profile, for which a chemical kinetics mechanism (Yao et al., 2017) is employed. In-depth calibration and validation of UVATZ was performed against experimental data from a marine RCCI engine (table 2). UVATZ was able to reproduce the in-cylinder pressure trace within a root mean square error (RMSE) of 0.85 bar to measurement and combustion performance indicators within a 5% error margin. Complete details regarding validation, and the modelling approach for UVATZ can be found in our previous work (Vasudev et al., 2022a).

As the current study is based on the same engine platform as used in Vasudev et al. (2022a), the calibrated UVATZ can be used to explore the design space. This methodology is well known within the engine research community, since multizone models (MZM) are capable of producing simulations with similar accuracy and predictivity to high fidelity CFD models, but at a fraction of the computational time (order of a few minutes). This unique ability of MZM, furthermore, explains its application in a wide range of engine research use cases, as described in (Vasudev et al., 2022b).

Briefly, the engine platform upon which the present approach is parameterized is a Wärtsilä "Mono" single-cylinder research engine (SCRE). This is a variant of the commercial W31 engine which is a multi-cylinder, dual-fuel, two-stage turbocharged power plant (Åstrand et al., 2016) operating on the lean-burn combustion of natural gas and diesel. The SCRE in the current research operates in RCCI mode, with natural gas (NG) as the low reactivity fuel and light fuel oil (LFO) as the high reactivity fuel. In terms of fuel metering, NG is administered via a multi-point system upstream of the intake valve, while LFO is direct injected via a twin-needle injector (Jay, 2016). Table 2 provides a brief summary of the specifications of this setup, while further details are presented in Vasudev et al. (2022a).

Table 2. Specifications of the Wärtsilä single cylinder research engine (SCRE)

Displacement	32.45 l
Nominal speed	720 rpm
Stroke/bore	1.39
Air system	External air compressor with air temperature & pressure control (up to 10 bar)
Valvetrain	4 valves with swirl + tumble ports variable intake valve closure (VIC) fixed exhaust valve opening (EVO)
Engine control	Rapid prototyping platform
Test fuels	ISO 8217 compliant LFO / LNG (MN=80)

2.5 Scope of research

Measurements from the SCRE include two steady-state RCCI operating points, which are used as baseline conditions in this research. OP A and B correspond to load points of 9 and 16 bar IMEP, respectively, as shown in table 3. The data is presented with respect to 'Ref', which is an IMO TIER III 25% load calibration point of the commercial W31DF engine. The dual fuel blend is quantified by blend ratio and is defined using NG on an energy basis, as in (3). The remaining parameter in table 3 is direct injection timing of the HRF (SOI_{LFO}).

Table 3. Steady-state measurement data. The baseline 'Ref' is the standard IMO TIER III 25% load calibration point on the commercial W31DF

OP	IMEP [bar]	BR [pp]	$SOI_{LFO}[CAD]$	λ [%]	T_{IVC} [K]
A	9	Ref -11	Ref -65	Ref +1.1	Ref +20
B	16	Ref -2.5	Ref -84.5	Ref -0.8	Ref +7.5

In addition to using OP A and B for validation of the RTM methodology, the points serve as nominal conditions upon which additional data for calibration is generated by simulating the validated UVATZ. This directly follows from the model-based development approach, thus enabling tailored sweeps of the most influential parameters to the RTM. Such an approach also enables the generation of quasi-transient data by assuming that inputs to UVATZ vary linearly between the steady-state measurement points. Table 4 presents this synthetically generated data. In the present work, the quantities λ, T_{IVC}, BR, and m_{EGR} are the fundamental independent variables, upon which the parameters in (4) are essentially based. It is worth noting that λ is defined with respect to the fuel mass. Cases 1-4 are sweeps of the aforementioned parameters on OP A, and case 8 is BR sweep on OP B. These cases were used for calibrating the MKIM. Cases 5-7 are sweeps performed varying two parameters at a time. Finally, case 9 is a quasi-transient sweep between OP A and B. It is worth mentioning that case 9 includes added noise to T_{IVC} and m_{EGR} in the input data.

Table 4. Operating conditions for calibration and validation of MKIM, RTM, and coupled RTM. Each test case corresponds to a sweep performed on the given parameters.

Case	IMEP [bar]	BR [%]	λ [-]	T_{IVC} [K]	m_{EGR} [g]	Validation
1	9	–	×	–	–	
2	9	–	–	×	–	
3	9	×	–	–	–	#o
4	9	–	–	–	×	
5	9	–	–	×	×	⋆
6	9	×	×	–	–	⋆
7	9	–	×	×	–	⋆
8	16	×	–	–	–	#o
9	9 → 16	×	×	×	×	⋆ o

⋆: tests performed for the MKIM validation. #: tests performed for the original RTM VS experimental data. o: tests utilized in this work for coupled RTM and MKIM model validation.

3. MODEL VALIDATION AND RESULTS

In this section, the aforementioned tests are presented and the validation results are discussed.

3.1 Validation of RTM

The full in-depth validation of the RTM can be found in the ongoing journal paper Storm (2023). Here, the validation results are presented by comparing the results with the UVATZ and experimental results, as indicated in table 3, case A and B.

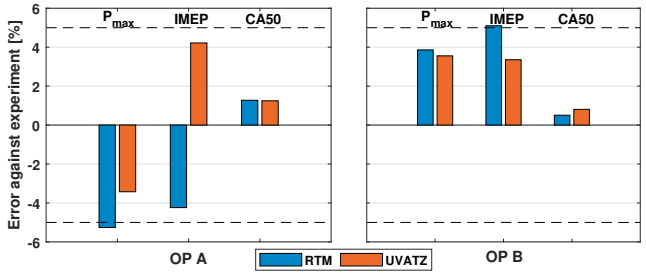

Fig. 3. RTM validation results compared with experimental results, dashed horizontal lines indicate the target accuracy of the UVATZ calibration.

The overall results show that the accuracy of UVATZ is within an error margin of 5% regarding the main combustion indicators: peak pressure (P_{max}), IMEP, and CA50. A similar result can be obtained with the RTM, where highest error is 5.2%, which is slightly beyond the error margin.

3.2 Calibration and validation of SOC model

The MKIM was optimized for two operating points with MATLAB's Global Optimization Toolbox. The operating points consist of mid and high engine load, as presented in table 3 and 4, respectively. The MKIM is optimized towards UVATZ. The value of CA10 was taken as a reference for the start of combustion. The MKIM predicted CA10 with a low error compared to both UVATZ and the experimental CA10, although it was not optimized towards the latter. The percent margin of error between the CA10 estimated by the MKIM and its UVATZ and experimental counterparts ispresented in table 5. The error between $CA10_{MKIM}$ and $CA10_{Experimental}$ is within a margin of 1%, while the margin of error for $CA10_{MKIM}$ and $CA10_{UVATZ}$

is less than 0.04% for all operating conditions. Hence, it can be concluded that the MKIM can predict SOC with low margins of error in steady-state conditions.

Table 5. Margin of error between $CA10_{experimental}$ and $CA10_{MKIM}$, and $CA10_{UVATZ}$ and $CA10_{MKIM}$, respectively.

OP	IMEP [bar]	$CA10_{error,\ UVATZ}$ [%]	$CA10_{error,\ Experimental}$ [%]
A	9	0.02	0.58
B	16	0.03	0.08

In Fig. 4, the correlation between CA10 and λ, T_{IVC}, BR, and m_{EGR} is shown for both UVATZ and the MKIM. The MKIM is able to estimate CA10 with a low margin of error while maintaining similar reaction as UVATZ. The increase of λ results in earlier combustion. The same can be seen in the increase of T_{IVC}. A higher BR and m_{EGR} on the other hand, result in later combustion, with an estimation error of 0.5 CAD compared to UVATZ. In these cases, the estimation error is less than 1 CAD, which occurs mostly outside nominal values.

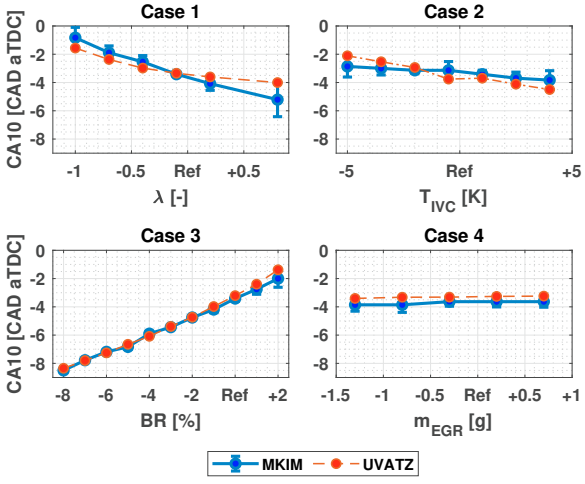

Fig. 4. Single parameter sweeps of MKIM compared to UVATZ in cases 1-4.

Similar behavior can be observed in multi-parameter sweeps, as shown in Fig. 5 and 6. In case 5, T_{IVC} and m_{EGR} exert an opposite effect on CA10. As already indicated in Fig. 4, a higher T_{IVC} results in earlier combustion and a higher m_{EGR} delays it. An increase in both parameters indicates earlier combustion. However, CA10 has a lower gradient, since the altered inputs exert opposite effects on CA10. In case 7, an increase of λ and T_{IVC} advances CA10, with both parameters reinforcing this effect. In both cases, estimation is less than 1 CAD for all points.

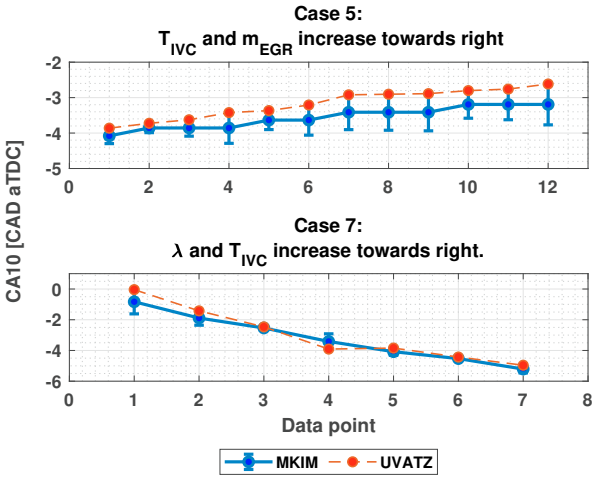

Fig. 5. Multi-parameter sweeps of MKIM compared to UVATZ in cases 5 and 7.

Case 6 contains multiple sweeps performed on BR and λ. In two cases, BR was kept constant outside the nominal value and the sweep was performed on λ (6a and 6b), and, in the other cases (6c and 6d), BR was changed in ascending and descending order, while λ was changed in ascending order. In case 6a, high BR delays the start of combustion. Conversely, a decrease in BR causes combustion to occur earlier. This can be seen from the start points of the trends in 6a and 6b. Increasing λ will advance the start of combustion as indicated earlier in the text. Moreover, with BR decreasing and λ increasing in case 6c, the start of combustion occurs earlier, while, in case 6d, the increase of BR delays combustion. This effect is similar to case 5. In all cases estimated CA10 has an error of less than 2 CAD.

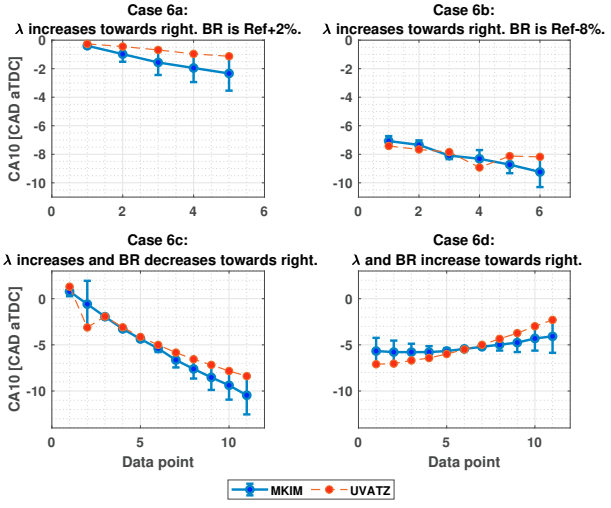

Fig. 6. Multi-parameter sweeps of MKIM compared to UVATZ in case 6.

Fig. 7 presents the CA10 at each point of case 9 for both the MKIM and UVATZ. The error is quite low during the entire sweep, with a slight increase outside nominal values, but, nevertheless, an error margin remaining at 1.5 CAD. It is worth mentioning that multi-parameter sweeps could also be considered transient sweeps, since the range of the chosen inputs overlaps both operating conditions.

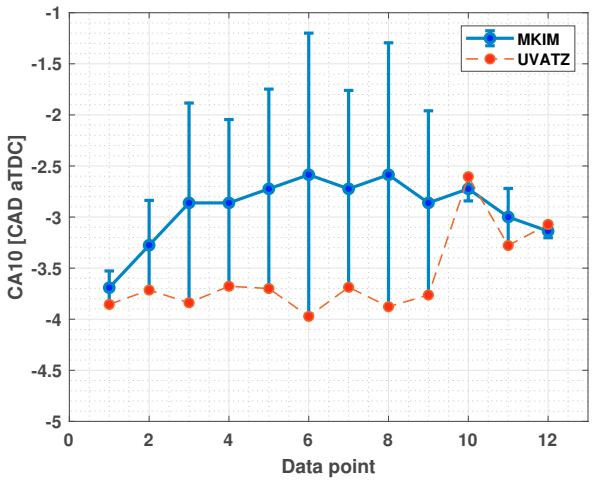

Fig. 7. Transient sweep of MKIM compared to UVATZ in case 9.

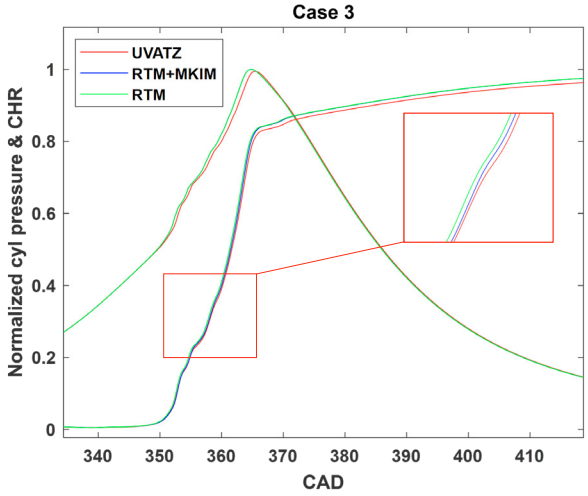

Fig. 8. CHR and cylinder pressure at cycle(k+1) for case 3.

The overall results indicate that the MKIM is capable of estimating CA10 with a low margin of error compared to UVATZ. Additionally, the MKIM displays similar behavior and sensitivity towards BR, λ, T_{IVC}, and m_{EGR} compared to UVATZ.

3.3 Validation of RTM embedded with SOC model

The coupled RTM and MKIM are validated against the experimentally validated UVATZ model. The test cases are described in table 4. Overall, the model is validated in three different conditions, which are at mid (10 cycles) and high load (8 cycles) with only BR changing, and a corresponding transient case (10 cycles) with both E_{fuel} and BR changing. The validation results are compared with the UVATZ results.

To provide an in-depth view of the trend-wise information, Fig. 8 describes the normalized CHR and cylinder pressure by the coupled RTM (in the figure RTM+MKIM), UVATZ, and the original RTM model (RTM) in test case 3. It can easily be seen that the CHR and cylinder pressure are estimated with good trend-wise accuracy from both the original RTM and the coupled RTM with the same amplitudes.

As mentioned earlier, the major improvement offered by the coupled RTM is the phasing of CHR; therefore, the amplitude remains the same. The zoomed-in region in Fig. 8 highlights the improved phasing of the coupled RTM compared to the original RTM. This is further demonstrated in Fig. 10 case 3, where the accuracy of CA10 is much better than that of the original RTM. Cylinder pressure, on the other hand, has a small error in phase, but the amplitude is correct.

The overall results from case 9 shown in Fig. 9 are similar to case 3, excellent trend-wise CHR is obtained, with only a slight mismatch of cylinder pressure phase. In transient case 9, the relatively higher errors stem from the fact that transient combustion is more challenging to estimate. In addition, the results are inaccurate in terms of CHR phasing, as indicated in Fig. 10 case 9, where slightly higher CA10 and CA50 errors are obtained from the coupled RTM. One key observation from the last two cycles is that the original RTM produces much higher error margins, due to its limitations, when the combustion is in the boundary region. For instance, here, the BR is extremely high, and this high BR pushes combustion to a boundary region where combustion changes extremely rapidly. As a result, chemical-driven combustion cannot be captured by the linear RTM; thus, accuracy falls. Nevertheless, the coupled RTM corrects this issue by applying the full predicative SOC model. In addition, the sensitivity to T_{IVC} and m_{EGR} from the MKIM improved the coupled model's reliability and applicable range significantly. Therefore, the errors from the coupled model in boundary conditions are much lower.

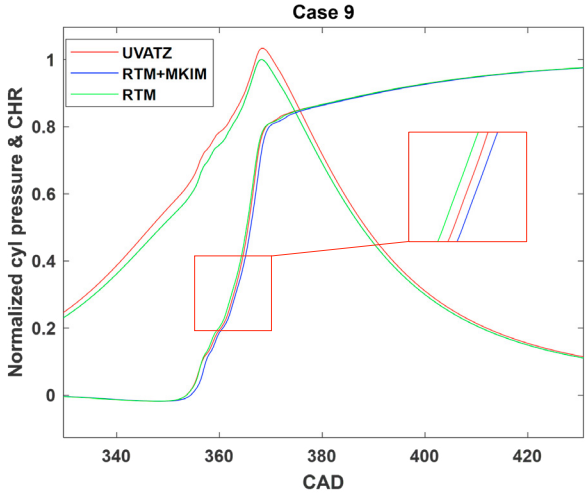

Fig. 9. CHR and cylinder pressure at cycle(k+1) for case 9.

Another issue revealed by the results is that CA50 generally has a higher error than CA10. This is due to the fact that shifting

CHR according to the SOC produces a more accurate CA10, so, for control application, this can be changed based on control design. For instance, when a more accurate CA50 is required, the shift can probably be based on the estimated CA50. To sum up, the coupled RTM model was able to achieve overall maximum errors for CA50 and CA10 of 1% and 1.2% in all three test cases, as shown in Fig. 10. As can be seen, the error results in test case 8 are the highest. This is because the MKIM is not fully optimized for this operating point compared to standalone RTM. This, in turn, demonstrates that coupled RTM combustion phasing estimation relies heavily on the accuracy of the MKIM.

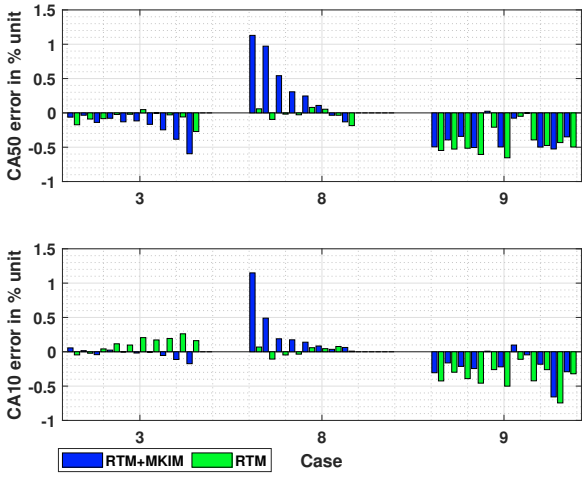

Fig. 10. CA10 and CA50 error in test cases 3, 8 and 9. Each error bar corresponds to a single cycle.

Nevertheless, the overall results indicate the predictability of the coupled RTM model with high trend-wise accuracy for CHR and cylinder pressure. In practice, pressure details cannot be accurately captured by a linear model. However, the combustion phasing parameters CA10 and CA50 can be estimated with excellent accuracy for control design. The automated and systematic SOC promotes the reliability of the RTM and overcomes the limitation from different combustion regions. The average cycle simulation time of standalone RTM, and coupled RTM and MKIM without any code optimization is around 5 ms and 20 ms, respectively. The simulation times were obtained using an Intel i7-11850H@2.5GHz processor (the rated speed of the 4-stroke engine is 750 rpm, which means 160 ms/cycle). Despite the increase of simulation time, this approach provides a promising model for conducting onboard MPC optimal control.

4. OUTLOOK

The SOC model applied in this work offers an ideal solution for a RCCI COM: simplifying the UVATZ model by applying a single zone approach and replacing chemical kinetics with the MKIM. In this way, real-time calculation capabilities can be feasible, and a fast and predictable RCCI COM is available for control design.

Our adaptive linear RTM model represents a viable solution for MPC control design considering its accuracy and cycle simulation time. The next step is to apply the model to RCCI MPC control design and prove the design tool chain through model in the loop (MIL) simulation.

5. CONCLUSION

This work demonstrated a successful upgrade of the linear time-varying RCCI RTM with a nonlinear SOC model capable of main combustion indicator accuracy of within 5% for RTM and of predicting both the common cycle-wise parameters and crank angle-based detailed combustion information. In addition, a maximum 1.5 CAD error from the highly accurate and comprehensive SOC model makes it an excellent match for a coupled RTM model, where model autonomy is improved dramatically. Overall, the innovative contributions of this work are as follows:

- The SOC model demonstrates similar behavior and sensitivity towards RCCI inputs to that of the reference UVATZ model. In general, the SOC model is able to estimate CA10 with a maximum error of 1.5 CAD compared to the UVATZ model. This makes it a good candidate for replacing the detailed chemical kinetics in the UVATZ and eventually realizing a fast RCCI COM. However, optimization of the MKIM requires improvements, since it is sensitive to initial conditions during the optimization procedure. This aspect will be investigated in future work. Nevertheless, this does not detract from the overall excellence of the SOC model's performance.
- The coupled RTM represents an automated and systematic linear model for MPC control design. This significantly improves model autonomy. The coupled RTM is able to improve the accuracy of combustion phasing estimation and enhance model reliability by covering even the boundary combustion region and providing full details of in-cylinder conditions. In addition, the coupled RTM covers a broad operating range, both in steady-state and transient conditions, with high fidelity.

ACKNOWLEDGEMENTS

This research is part of the Clean Propulsion Technologies project (CPT) funded by Business Finland. The experimental data was provided by Wärtsilä Oyj Abp. We would also like to express our gratitude to Mr. Matthew Billington, for his invaluable contribution in proofreading this work and providing his expert suggestions on stylistic points.

REFERENCES

Albin Rajasingham, T. (2021). *Introduction. In: Nonlinear Model Predictive Control of Combustion Engines*. Springer. doi:10.1007/978-3-030-68010-7_1.

Arnberger, A., Golini, S., Mumford, D., and Hasenbichler, G. (2018). Commercial natural gas vehicles: tomorrow's engine technologies for most stringent nox and co2 targets. In J. Liebl, C. Beidl, and W. Maus (eds.), *Internationaler Motorenkongress 2018*, 315–338. Springer Fachmedien Wiesbaden, Wiesbaden.

Åstrand, U., Aatola, H., and Myllykoski, J. (2016). Wärtsilä 31-worlds most efficient fourstroke engine. In *CIMAC Congress Helsinki, Paper*, volume 225.

Basina, L.N.A., Irdmousa, B.K., Velni, J.M., Borhan, H., Naber, J.D., and Shahbakhti, M. (2020). Data-driven modeling and predictive control of maximum pressure rise rate in rcci engines. In *2020 IEEE Conference on Control Technology and Applications (CCTA)*, 94–99. doi:10.1109/CCTA41146.2020.9206358.

Benajes, J., Pastor, J.V., García, A., and Monsalve-Serrano, J. (2015). The potential of rcci concept to meet euro vi

nox limitation and ultra-low soot emissions in a heavy-duty engine over the whole engine map. *Fuel*, 159, 952–961. doi:10.1016/j.fuel.2015.07.064.

De Ojeda, W., Zhang, Y., Xie, K., Han, X., Wang, M., and Zheng, M. (2012). Exhaust hydrocarbon speciation from a single-cylinder compression ignition engine operating with in-cylinder blending of gasoline and diesel fuels. Technical report. doi:10.4271/2012-01-0683.

Irdmousa, B.K., Rizvi, S.Z., Veini, J.M., Nabert, J.D., and Shahbakhti, M. (2019). Data-driven modeling and predictive control of combustion phasing for rcci engines. In *2019 American Control Conference (ACC)*, 1617–1622. doi:10.23919/ACC.2019.8815269.

Irdmousa, B.K., Naber, J.D., Velni, J.M., Borhan, H., and Shahbakhti, M. (2021). Input-output data-driven modeling and mimo predictive control of an rcci engine combustion. *IFAC-PapersOnLine*, 54, 406–411. doi:https://doi.org/10.1016/j.ifacol.2021.11.207.

Jay, D. (2016). Cr development in the last decade in wärtsilä. In *28th CIMAC Congress Helsinki, Paper*, volume 232.

Kakoee, A., Bakhshan, Y., Barbier, A., Bares, P., and Guardiola, C. (2020). Modeling combustion timing in an rcci engine by means of a control oriented model. *Control Engineering Practice*, 97, 104321. doi:10.1016/j.conengprac.2020.104321.

Kondipati, N.N.T., Arora, J.K., Bidarvatan, M., and Shahbakhti, M. (2017). Modeling, design and implementation of a closed-loop combustion controller for an rcci engine. In *2017 American Control Conference (ACC)*, 4747–4752. doi:10.23919/ACC.2017.7963689.

Livengood, J. and Wu, P. (1955). Correlation of autoignition phenomena in internal combustion engines and rapid compression machines. *Symposium (International) on Combustion*, 5(1), 347–356. doi:10.1016/S0082-0784(55)80047-1.

Mikulski, M., Ramesh, S., and Bekdemir, C. (2019). Reactivity controlled compression ignition for clean and efficient ship propulsion. *Energy*, 182, 1173–1192. doi:10.1016/j.energy.2019.06.091.

Mishra, C. and Subbarao, P.M.V. (2021). A comparative study of physics based grey box and neural network trained black box dynamic models in an rcci engine control parameter prediction. In *SAE WCX Digital Summit*. SAE International. doi:10.4271/2021-01-0178.

Raut, A., Irdmousa, B., and Shahbakhti, M. (2018). Dynamic modeling and model predictive control of an rcci engine. *Control Engineering Practice*, 81, 129–144. doi:10.1016/j.conengprac.2018.09.004.

Reitz, R.D. and Duraisamy, G. (2015). Review of high efficiency and clean reactivity controlled compression ignition (rcci) combustion in internal combustion engines. *Progress in Energy and Combustion Science*, 46, 12–71. doi:10.1016/j.pecs.2014.05.003.

Sadabadi, K. (2015). *MODELLING AND CONTROL OF COMBUSTION PHASING OF AN RCCI ENGINE*. Master's thesis, Michigan Technological University. doi:10.37099/mtu.dc.etds/966.

Sadabadi, K.K., Shahbakhti, M., Bharath, A.N., and Reitz, R.D. (2016). Modeling of combustion phasing of a reactivity-controlled compression ignition engine for control applications. *International Journal of Engine Research*, 17(4), 421–435. doi:10.1177/1468087415583773.

Shahbakhti, M. (2009). *Modeling and experimental study of an HCCI engine for combustion timing control*. Ph.D. thesis, University of Alberta. doi:10.7939/R3PG8X.

Splitter, D., Hanson, R., Kokjohn, S., and Reitz, R.D. (2011). Reactivity controlled compression ignition (rcci) heavy-duty engine operation at mid-and high-loads with conventional and alternative fuels. In *SAE World Congress & Exhibition*. SAE International. doi:10.4271/2011-01-0363.

Storm, X. (2023). Development of a real-time linear rcci model for combustion control design. *Control Engineering Practice*.

Turesson, G. (2018). *Model-Based Optimization of Combustion-Engine Control*. Ph.D. thesis, Lund University. doi:10.13140/RG.2.2.36319.97440.

Vasudev, A., Cafari, A., Axelsson, M., Mikulski, M., and Hyvonen, J. (2022a). Towards next generation control-oriented thermo-kinetic model for reactivity controlled compression ignition marine engines. In *SAE Powertrains, Fuels & Lubricants Conference & Exhibition*. SAE International. doi:10.4271/2022-01-1033.

Vasudev, A., Mikulski, M., Balakrishnan, P.R., Storm, X., and Hunicz, J. (2022b). Thermo-kinetic multi-zone modelling of low temperature combustion engines. *Progress in Energy and Combustion Science*, 91, 100998. doi:10.1016/j.pecs.2022.100998.

Yao, T., Pei, Y., Zhong, B.J., Som, S., Lu, T., and Luo, K.H. (2017). A compact skeletal mechanism for n-dodecane with optimized semi-global low-temperature chemistry for diesel engine simulations. *Fuel*, 191, 339–349. doi:10.1016/j.fuel.2016.11.083.